

A unitary perturbation theory approach to real-time evolution problems

This article has been downloaded from IOPscience. Please scroll down to see the full text article.

2009 J. Phys.: Condens. Matter 21 015601

(<http://iopscience.iop.org/0953-8984/21/1/015601>)

View [the table of contents for this issue](#), or go to the [journal homepage](#) for more

Download details:

IP Address: 129.252.86.83

The article was downloaded on 29/05/2010 at 16:54

Please note that [terms and conditions apply](#).

A unitary perturbation theory approach to real-time evolution problems

A Hackl¹ and S Kehrein²

¹ Institut für Theoretische Physik, Universität zu Köln, Zùlpicher Straße 77, 50937 Köln, Germany

² Arnold Sommerfeld Center for Theoretical Physics and CeNS, Department für Physik, Ludwig-Maximilians-Universität, Theresienstrasse 37, 80333 München, Germany

E-mail: ah@thp.uni-koeln.de

Received 20 September 2008, in final form 23 October 2008

Published 1 December 2008

Online at stacks.iop.org/JPhysCM/21/015601

Abstract

We discuss a new analytical approach to real-time evolution in quantum many-body systems. Our approach extends the framework of continuous unitary transformations such that it amounts to a novel solution method for the Heisenberg equations of motion for an operator. It is our purpose to illustrate the accuracy of this approach by studying dissipative quantum systems on all timescales. In particular, we obtain results for non-equilibrium correlation functions for general initial conditions. We illustrate our ideas for the exactly solvable dissipative oscillator and, as a non-trivial model, for the dissipative two-state system.

1. Introduction

Strongly correlated many-body systems are challenging due to their highly non-trivial interplay between different energy scales. In experiment, many of their properties are probed by measuring their linear response to weak external driving forces. An additional branch of physical phenomena is currently being explored by driving quantum many-body systems far out of equilibrium and studying such new states of matter. In particular, recent progress in atomic physics has made it possible to tune systems of ultracold atoms at will between different interacting regimes. For example, a seminal experiment by Greiner *et al* [1] shows collapse and revival phenomena in atomic Bose gases after an interaction quench, where excellent isolation from the environment allows the observation of such non-equilibrium behavior at remarkably long timescales.

From the theoretical side, non-equilibrium quantum systems are very challenging since many well-established methods from equilibrium physics cannot be directly applied. Significant progress has been achieved in low-dimensional systems and for quantum impurity systems with numerical methods such as numerical renormalization group (NRG) and density matrix renormalization group (DMRG): their newly developed extensions called time-dependent density matrix renormalization group (TD-DMRG) [2] and time-dependent numerical renormalization group (TD-NRG) [3, 4], were, for

example, successfully applied to interaction quenches in the Bose–Hubbard model [5] and to impurity spins coupled to bosonic or fermionic baths [4]. More recent applications of these methods also include interaction quenches in fermionic lattice systems in one dimension [6] and the calculation of steady state currents through nano-devices [7].

The extension of conventional analytical techniques seems to be more difficult. For example, the renormalization group approach, which is designed to construct effective low energy Hamiltonians, is not ideally suited to understanding non-equilibrium situations, where energy scales well above the low energy sector can be excited. The situation is not much better in weakly interacting systems, where diagrammatic expansions are usually the first tool to analyze ground states and their elementary excitations, and often yield reliable results in thermal equilibrium. Nevertheless, even in weakly interacting systems, perturbation theory is often not capable of describing the long-time behavior of non-equilibrium observables, since truncation errors can become uncontrolled at large timescales.

In this paper, we present a new analytical approach to the real-time evolution problem which merges the advantages of perturbation theory and renormalization group theory, and at the same time leaves behind their shortcomings mentioned above. In two short previous publications, this approach has already been introduced and was applied to two different problems [8, 9]. Here we give a somehow more pedagogical introduction, provide more details, and discuss its general

applicability to the field of dissipative quantum systems. In the last 20 years, quantum physics in a dissipative environment has played an important role in solid state physics, quantum optics, quantum computing, chemical, and even biological systems (for a review, see [12, 13]). In addition, this field is especially suitable for checking the accuracy of our approximation scheme since many results from other approaches are known. However, our approach is applicable to a much wider class of problems, including also lattice models, see for example [9].

1.1. Summary of results

Our approach is based on an analogy to canonical perturbation theory in classical mechanics. We give a simple illustration of canonical perturbation theory and show how canonical transformations can improve perturbative expansions in real-time evolution problems. We show that an analogous implementation for quantum many-body systems is possible, based on Wegner's flow equation approach [10]. Independently, the same approach has been developed in the field of high energy physics [11]. Using this approach, we reproduce the exact solution for a quantum dissipative oscillator and show that efficient and precise numerical solutions of the analytical equations can be obtained. We also illustrate the failure of naive perturbation theory in this simple quantum mechanical system.

For the spin-boson model, we obtain results that are in excellent agreement with known results. In the regime of weak coupling to the bath, we reproduce exact results for the decoherence of a spin without tunnel splitting. For finite tunnel splitting, we calculate the non-equilibrium correlation function of the spin projection and also obtain the quantitatively correct coherent decay of the spin polarization in the weakly damped ohmic regime.

1.2. Outline

In section 2 we give an introduction to the basic ideas of our method and its technical details. First we motivate our approach using an analogy from classical mechanics. Then we discuss the method in detail. In section 3, we apply this approach to a simple exactly solvable model which is useful to understand the technical details of our method. In section 4, we apply our method to the non-trivial spin-boson model to analyze the reliability of our approximation scheme. A brief summary and outlook concludes the paper in section 5.

2. Real-time evolution with the flow equation method

2.1. Motivation: canonical perturbation theory in classical mechanics

There exist well-established methods to handle time-dependent perturbations in classical mechanics, and early attempts to handle these problems date back even to Newton [14], who considered the small distortion of the moon's orbit caused by the gravitational force of the sun.

Much progress in this field has been motivated by the ever increasing accuracy of observational data for planetary

motion and satellites, and the need to make accurate predictions based on this. The common approaches to these problems are collectively summarized as 'canonical perturbation theory' [14]. The basic idea behind canonical perturbation theory can be simply illustrated by the Hamilton function of a weakly perturbed classical harmonic oscillator,

$$H = \frac{1}{2}p^2 + \frac{1}{2}q^2 + \frac{g}{4}q^4, \quad (1)$$

where a quartic anharmonic term with a small coupling $g \ll 1$ perturbs the trajectory. We consider the initial conditions $q(t=0) = 0$ and $p(t=0) = v + \frac{3}{8}gv^3$ in the following.

By exploiting the smallness of the quartic perturbation, one might be tempted to employ naive perturbation theory which uses a series in powers of g as an ansatz for the perturbed solution $q(t)$,

$$q(t) = q^{(0)}(t) + gq^{(1)}(t) + O(g^2). \quad (2)$$

The trajectory $q^{(0)}(t)$ is just the solution of the unperturbed problem,

$$q^{(0)}(t) = v \sin(t). \quad (3)$$

From Hamilton's equations,

$$\frac{\partial H}{\partial p} = \dot{q}; \quad \frac{\partial H}{\partial q} = -\dot{p}, \quad (4)$$

we obtain the equation of motion

$$\ddot{q}^{(1)}(t) = -q^{(1)}(t) - v^3 \sin^3(t), \quad (5)$$

which has the solution

$$q^{(1)}(t) = \frac{3}{8}v^3 \sin(t) - \frac{v^3}{8}(\sin(t) \cos^2(t) + 2 \sin(t) - 3t \cos(t)). \quad (6)$$

This result already reveals the caveat of this approach, since the so-called secular term $3t \cos(t)$ yields an error growing unbounded in time. In fact, it is a well-known general result from classical mechanics that such secular terms invalidate naive perturbation theory for large times.

Naive perturbation theory can be much improved in the framework of canonical perturbation theory. This approach first transforms the Hamilton function to a suitable normal form, and after solving the equations of motion in this canonical basis, the normal coordinates are reexpressed through the old coordinates. In this manner secular terms can be avoided. To implement this idea, we first look for a canonical transformation of variables

$$(q, p) \rightarrow (Q, P) \quad (7)$$

that brings the Hamilton function to the following normal form, denoted by \tilde{H} ,

$$\tilde{H} = H_0 + g\alpha H_0^2 + O(g^2) \quad \text{with } H_0 = \frac{1}{2}P^2 + \frac{1}{2}Q^2. \quad (8)$$

It is easy to see that the Poisson bracket $\{H_0, H_0^2\}$ vanishes, hence the equations of motion for Q and P can be

solved trivially. These variables obey the initial conditions $Q(0) = 0$ and $P(0) = 0$. In our example, the corresponding transformation of variables is

$$\begin{aligned} q(t) &= Q(t) - \frac{3}{32}g (3P^2(t)Q(t) + \frac{5}{3}Q^3(t)) + O(g^2), \\ p(t) &= P(t) + \frac{3}{32}g (5P(t)Q^2(t) + P^3(t)) + O(g^2) \end{aligned} \quad (9)$$

which is performed perturbatively in the parameter g . The normal form (8) has been chosen such that the equation of motion for the new variables $P(t)$ and $Q(t)$ can now be solved exactly, without producing any secular term. Using this strategy, the final result is

$$\begin{aligned} q(t) &= v \sin(\omega t) - \frac{3}{32}g v^3 (3 \cos^2(\omega t) \sin(\omega t) + \frac{5}{3} \sin^3(\omega t)) \\ &\quad + O(g^2), \\ p(t) &= v \cos(\omega t) + \frac{3}{32}g v^3 (5 \sin^2(\omega t) \cos(\omega t) + \cos^3(\omega t)) \\ &\quad + O(g^2) \end{aligned} \quad (10)$$

where $\omega = 1 + \frac{3}{4}g E_0$ and $E_0 = p(0)^2/2$. We show a comparison of naive perturbation theory and canonical perturbation theory in figure 1, which demonstrates the usefulness of canonical perturbation theory.

Canonical perturbation theory yields renormalized parameters of the unperturbed problem, but does not lead to secular terms. This improvement becomes directly visible by expanding the contribution $\sin(\omega t)$ in powers of g ,

$$\begin{aligned} \sin(\omega t) &= \sin\left(\left(1 + \frac{3}{4}g E_0\right) t\right) \\ &= \sin(t) + \frac{3}{4}g E_0 t \cos(t) + O(g^2). \end{aligned} \quad (12)$$

This expansion generates the secular term from equation (6) occurring in naive perturbation theory, making it obvious that canonical perturbation theory contains a summation over secular terms which in total yield a much improved result in comparison to naive perturbation theory. Notice that this is true in spite of the fact that *both approaches have been expanded to the same power in the small coupling constant*.

2.2. Perturbation theory in non-equilibrium quantum mechanics

In quantum many-body systems, the canonical way to evaluate the real-time evolution of observables starting from some non-thermal initial state is the Keldysh technique [15], which defines a contour ordered S -matrix in order to develop perturbative expansions for non-equilibrium Green functions. Just as in our example of naive perturbation theory, secular terms can occur in any finite order of perturbation theory, and there is no universal solution for how to sum up these secular terms. These difficulties can make it very difficult or even impossible to study the transient evolution of observables into a steady state.

One might wonder why an analogue of canonical perturbation theory for quantum many-body systems had not been developed earlier. The basic reason is the notorious difficulty in transforming quantum many-body systems into normal form. In addition, the continuum of energy scales often causes often non-perturbative effects in coupling constants. Since the advent of renormalization group techniques, the

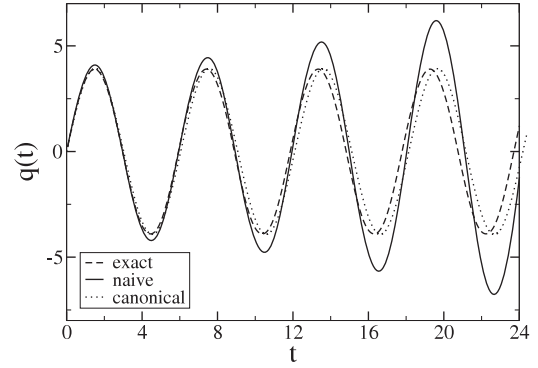


Figure 1. We compare the different approaches to solve the equations of motion for the anharmonic oscillator from equation (1). The difference between the numerically exact solution and canonical perturbation theory according to equation (11) can hardly be noticed. Naive perturbation theory already yields large errors after a few oscillations, with an error that grows linearly in time t . Our parameters are $v = 4$ and coupling strength $g = 0.01$.

much easier problem of constructing effective low energy theories has attracted most of the attention. The more general problem of constructing normal forms of interacting Hamiltonians has been successfully treated only during the last few years.

2.3. Flow equation approach

A general description of how to transform interacting quantum many-body systems into a non-interacting normal form was given in 1994 by Wegner [10]. Let us briefly review the basic ideas of the flow equation approach (for more details see [17]). A many-body Hamiltonian H is diagonalized through a sequence of infinitesimal unitary transformations with an anti-Hermitian generator $\eta(B)$,

$$\frac{dH(B)}{dB} = [\eta(B), H(B)], \quad (13)$$

with $H(B = 0)$ the initial Hamiltonian. The ‘canonical’ generator [10] is the commutator of the diagonal part H_0 with the interaction part H_{int} of the Hamiltonian, $\eta(B) \stackrel{\text{def}}{=} [H_0(B), H_{\text{int}}(B)]$. It can be formally shown that the choice of the canonical generator is by construction suitable to eliminate interaction matrix elements with energy transfer $\Delta E = O(1/\sqrt{B})$. Under rather general conditions, an increasingly energy-diagonal Hamiltonian is obtained. For $B = \infty$ the Hamiltonian will be energy diagonal and we denote parameters and operators in this basis by $\tilde{\cdot}$, e.g. $\tilde{H} = H(B = \infty)$.

Usually, this scheme cannot be implemented exactly. The generation of higher and higher order interaction terms in (13) makes it necessary to truncate the scheme in some order of a suitable systematic expansion parameter (usually the running coupling constant). Still, the infinitesimal nature of the approach makes it possible to deal with a continuum of energy scales and to describe non-perturbative effects. This has led to numerous applications of the flow equation method where one utilizes the fact that the Hilbert space is not truncated as opposed to conventional scaling methods.

In [8], these features have been exploited in order to develop an analogue of canonical perturbation theory in classical mechanics for quantum many-body systems. The general setup is described by the diagram in figure 2, where $|\Psi_i\rangle$ is some initial non-thermal state whose time evolution one is interested in. However, instead of following its full-time evolution it is usually more convenient to study the real-time evolution of a given observable A that one is interested in. This is done by transforming the observable into the diagonal basis in figure 2 (*forward transformation*):

$$\frac{dO}{dB} = [\eta(B), O(B)] \quad (14)$$

with the initial condition $O(B=0) = A$. The key observation is that one can now solve the real-time evolution with respect to the energy diagonal \tilde{H} exactly, thereby avoiding any errors that grow proportional to time (i.e. secular terms): this yields $\tilde{A}(t)$. Now since the initial quantum state is given in the $B = \infty$ basis, one undoes the basis change by integrating (14) from $B = \infty$ to $B = 0$ (*backward transformation*) with the initial condition $O(B = \infty) = \tilde{A}(t)$. One therefore effectively generates a new non-perturbative scheme for solving the Heisenberg equations of motion for an operator, $A(t) = e^{iHt} A(0) e^{-iHt}$, in exact analogy to canonical perturbation theory.

3. The dissipative harmonic oscillator

The dissipative harmonic oscillator is a widely used toy model in the field of quantum optics and is also used in many other contexts [16]. It describes a quantum oscillator of frequency Δ coupled linearly to a heat bath consisting of bosonic normal modes b_k .

$$H = \Delta b^\dagger b + \sum_k \omega_k b_k^\dagger b_k + E_0 + \sum_k \lambda_k (b + b^\dagger)(b_k + b_k^\dagger). \quad (15)$$

The operators b_k fulfil canonical commutation relations

$$[b_k, b_{k'}^\dagger] = \delta_{kk'} \quad (16)$$

and their influence on the physical properties of the quantum oscillator can be fully described by the spectral function

$$J(\omega) \stackrel{\text{def}}{=} \sum_k \lambda_k^2 \delta(\omega - \omega_k). \quad (17)$$

In experiment, the high frequency part of $J(\omega)$ only affects the short time-response of the system, and thus, this part of the spectrum is usually cut off from $J(\omega)$. In consequence, the function $J(\omega)$ is commonly approximated by a power-law behavior $J(\omega) \propto \omega^s$, $\omega < \omega_c$. Three different regimes of the exponent are distinguished, for $0 < s < 1$ the bath is called ‘subohmic’, for $s = 1$ the bath is called ‘ohmic’, and for $s > 1$ ‘superohmic’.

We imagine that the system is prepared in a well-defined quantum state at some time t_0 and the subsequent real-time evolution of physical quantities is then defined by the Hamiltonian (15). The flow equation method does not restrict the class of possible initial states, but in this work we will

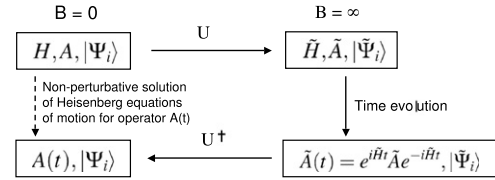


Figure 2. How to make use of the flow equation method to implement the analogue of canonical perturbation theory in quantum mechanics. U denotes the full unitary transformation that relates the $B = 0$ to the $B = \infty$ basis.

consider the system-bath complex at time $t = 0$ to be prepared in a product state

$$|\alpha\rangle \otimes |\Omega\rangle \quad (18)$$

with the quantum oscillator in a coherent state

$$|\alpha\rangle = e^{-\frac{a^2}{2}} \sum_{n=0}^{\infty} \frac{a^n}{\sqrt{n!}} |n\rangle, \quad a \in \mathbb{R} \quad (19)$$

and the heat bath in the bosonic vacuum state $|\Omega\rangle$. In such a state, the displacement $\langle \hat{x} \rangle = 1/\sqrt{2} \langle (b + b^\dagger) \rangle$ will be finite and the effects of decoherence and dissipation will manifest themselves in the real-time evolution of the observable $\langle \hat{x}(t) \rangle$. The flow equation method, outlined in section 2, can solve this problem exactly without approximations. First, the flow equations for the Hamiltonian are derived. Then the real-time evolution of the operators b and b^\dagger is implemented by their time-dependent flow equations. This will allow us to study the forward-backward transformation scheme in the context of an exactly solvable model.

3.1. Diagonalization of the Hamiltonian

As the first step of our program, the coupled form of the Hamiltonian (15) will be diagonalized by infinitesimal unitary transformations. Due to the quadratic nature of the Hamiltonian (15), the flow equations for the Hamiltonian can be derived in closed form, as shown in [19].

Commuting the interaction part with the non-interacting boson part of (15) yields the canonical generator $\eta(B) = [\Delta b^\dagger b + \sum_k \omega_k b_k^\dagger b_k, \sum_k \lambda_k (b + b^\dagger)(b_k + b_k^\dagger)]$ of unitary transformations:

$$\begin{aligned} \eta(B) &= \sum_k \lambda_k(B) \Delta(B) (b^\dagger - b)(b_k + b_k^\dagger) \\ &+ \sum_k \omega_k(B) \lambda_k(B) (b + b^\dagger)(b_k - b_k^\dagger). \end{aligned} \quad (20)$$

This generator leads to additional terms in the flowing Hamiltonian that violate the form invariance of equation (15). The flowing Hamiltonian preserves its initial form if the generator is extended by additional terms. In the following, we omit the explicit dependence of coefficients on the parameter B .

$$\begin{aligned} \eta(B) &= \sum_k \eta_k^{(1)} (b - b^\dagger)(b_k + b_k^\dagger) \\ &+ \sum_{k,q} \omega_k \lambda_k (b + b^\dagger)(b_k - b_k^\dagger) \\ &+ \sum_{k,q} \eta_{k,q} (b_k + b_k^\dagger)(b_q - b_q^\dagger) + \eta_b (b^2 - b^{\dagger 2}) \end{aligned} \quad (21)$$

with the coefficients

$$\begin{aligned}\eta_k^{(1)} &= -\lambda_k \Delta \tilde{f}(\omega_k, B) \\ \eta_k^{(2)} &= \lambda_k \omega_k \tilde{f}(\omega_k, B) \\ \eta_{k,q} &= -\frac{2\lambda_k \lambda_q \Delta \omega_q}{\omega_k^2 - \omega_q^2} (\tilde{f}(\omega_k, B) + \tilde{f}(\omega_q, B)) \\ \eta_b &= -\frac{1}{4\Delta} \frac{d\Delta}{dB}\end{aligned}\quad (22)$$

which are chosen such that they leave the flowing Hamiltonian form invariant. For this purpose the function $\tilde{f}(\omega_k, B)$ is still arbitrary, except for the obvious requirement $\lambda_k(B = \infty) = 0$. For our numerical evaluations of the flow equations later on, we will chose $\tilde{f}(\omega_k, B) = -\frac{\omega_k - \Delta}{\omega_k + \Delta}$, which leads to good convergence properties in the limit $B \rightarrow \infty$.

The flowing parameters of the transformed Hamiltonian are governed by the coupled differential equations

$$\begin{aligned}\frac{d\Delta(B)}{dB} &= 4 \sum_k \eta_k^{(2)} \lambda_k \\ \frac{dE_0(B)}{dB} &= 2 \sum_k \eta_k^{(2)} \lambda_k + 2 \sum_k \eta_k^{(1)} \lambda_k \\ \frac{d\omega_k}{dB} &= O\left(\frac{1}{N}\right) \\ \frac{d\lambda_k}{dB} &= \Delta \eta_k^{(1)} + \omega_k \eta_k^{(2)} + 2 \sum_q \eta_{k,q} \lambda_q + 2\eta_b \lambda_k.\end{aligned}\quad (23)$$

The renormalization of the bath frequencies ω_k will have a vanishing effect on time-dependent observables in the thermodynamic limit $N \rightarrow \infty$. Therefore, the flow equations of these energies can be ignored for our purposes. In the limit $B \rightarrow \infty$, the Hamiltonian is diagonalized and the tunneling matrix element Δ is renormalized to some value $\tilde{\Delta}$.

$$\tilde{H} = \tilde{\Delta} b^\dagger b + \sum_k \omega_k b_k^\dagger b_k. \quad (24)$$

In order to proceed with the real-time evolution of observables, the second step of the program outlined in section 2 requires the analogous transformation of the system operators.

The flow of the bosonic operator $b(B)$ is determined by the generator (21) and yields the following structure

$$\begin{aligned}b(B) &= \beta(b + b^\dagger) + \tilde{\beta}(b - b^\dagger) \\ &+ \sum_k \alpha_k (b_k + b_k^\dagger) + \tilde{\alpha}_k (b_k - b_k^\dagger)\end{aligned}\quad (25)$$

with the flow equations

$$\begin{aligned}\frac{d\beta(B)}{dB} &= 2\eta_b \beta + 2 \sum_k \alpha_k \eta_k^{(2)} \\ \frac{d\tilde{\beta}(B)}{dB} &= -2\eta_b \tilde{\beta} - 2 \sum_k \tilde{\alpha}_k \eta_k^{(1)} \\ \frac{d\alpha_k(B)}{dB} &= 2\eta_k^{(1)} + 2 \sum_q \eta_{k,q} \alpha_q \\ \frac{d\tilde{\alpha}_k(B)}{dB} &= -2\eta_k^{(2)} \tilde{\beta} - 2 \sum_q \eta_{q,k} \tilde{\alpha}_q.\end{aligned}\quad (26)$$

The initial conditions are $\beta(B = 0) = \tilde{\beta}(B = 0) = 1/2$, $\alpha_k(B = 0) = \tilde{\alpha}_k(B = 0) = 0$. During the flow towards $B \rightarrow \infty$, the operator b changes its structure into a complicated superposition of bath operators.

3.2. Real-time evolution in closed form

It is now easy to formulate an exact transformation that yields the operator $b(t)$, $t > 0$, which is time evolved with respect to the Hamiltonian (15). First, the operator \tilde{b} is trivially time evolved with respect to the Hamiltonian (24) as

$$\tilde{b}(t) \stackrel{\text{def}}{=} e^{i\tilde{H}t} \tilde{b} e^{-i\tilde{H}t}.$$

This operation endows the coefficients in (25) with trivial phase factors

$$\begin{aligned}\tilde{\beta}(t) &\stackrel{\text{def}}{=} \tilde{\beta} \cos(\tilde{\Delta}t) - i\tilde{\beta} \sin(\tilde{\Delta}t) \\ \tilde{\tilde{\beta}}(t) &\stackrel{\text{def}}{=} \tilde{\tilde{\beta}} \cos(\tilde{\Delta}t) - i\tilde{\tilde{\beta}} \sin(\tilde{\Delta}t) \\ \tilde{\alpha}_k(t) &\stackrel{\text{def}}{=} \tilde{\alpha}_k \cos(\omega_k t) - i\tilde{\alpha}_k \sin(\omega_k t) \\ \tilde{\tilde{\alpha}}_k(t) &\stackrel{\text{def}}{=} \tilde{\tilde{\alpha}}_k \cos(\omega_k t) - i\tilde{\tilde{\alpha}}_k \sin(\omega_k t)\end{aligned}\quad (27)$$

leading to the operator

$$\begin{aligned}\tilde{b}(t) &= \tilde{\beta}(t)(b + b^\dagger) + \tilde{\tilde{\beta}}(t)(b - b^\dagger) + \sum_k \tilde{\alpha}_k(t)(b_k + b_k^\dagger) \\ &+ \sum_k \tilde{\tilde{\alpha}}_k(t)(b_k - b_k^\dagger).\end{aligned}\quad (28)$$

The second step is to obtain the operator $b(t)$ from the operator $\tilde{b}(t)$ by reverting the unitary transformation³ U used to diagonalize the Hamiltonian (15), formally represented by the relation $b(t) = U^\dagger \tilde{b}(t) U$. For this purpose, we again make an ansatz for the flow of the operator $\tilde{b}(t)$

$$\begin{aligned}b(B, t) &= \beta(B, t)(b + b^\dagger) + \tilde{\beta}(B, t)(b - b^\dagger) \\ &+ \sum_k \tilde{\alpha}_k(B, t)(b_k + b_k^\dagger) + \tilde{\tilde{\alpha}}_k(B, t)(b_k - b_k^\dagger),\end{aligned}\quad (29)$$

where all coefficients have both real and imaginary parts, since the initial conditions at $B = \infty$ are given by the complex valued expressions from (27). Since the ansatz of equation (29) is formally identical to that of (25), the unitary flow of $b(B, t)$ can again be calculated by using the flow equations (26). The operator $b(t)$ is now obtained by integrating the flow equations (26) from $B = \infty$ to 0, using the parameters from (29) and the initial conditions for $B = \infty$, as given by equations (27). Since all transformations are unitary, the operator $b^\dagger(t)$ is readily obtained by the Hermitian conjugate of equation (29).

All transformations used up to now do not depend on the initial state of the quantum system. In calculations of time-dependent physical quantities, the operator $b(t)$ can be evaluated with respect to equilibrium heat baths at finite temperature as well as arbitrary non-equilibrium ensembles.

³ The full unitary transformation U can be expressed as a B -ordered exponential, $U = T_B \exp(\int_0^\infty \eta(B) dB)$. However, this expression is only formally useful since it cannot be evaluated without additional approximations.

3.3. Analytical results

3.3.1. Naive perturbation theory. In analogy to classical perturbation theory as discussed in the introduction, a perturbative result for quantum evolution can be obtained by directly expanding the Heisenberg equation of motion for an operator. The exact time evolution of the operator $\hat{x} = (b + b^\dagger)/\sqrt{2}$ is

$$\hat{x}(t) = e^{iHt} \hat{x} e^{-iHt}, \quad (30)$$

where H is given by equation (15). A perturbative expansion of equation (30) is typically performed in the interaction picture, which we define by

$$\hat{x}_I(t) = e^{-iH_0 t} \hat{x}(t) e^{iH_0 t}, \quad (31)$$

and $H_0 = \Delta b^\dagger b + \sum_k \omega_k b_k^\dagger b_k$ is the non-interacting part of the Hamiltonian. Equation (31) leads to the equation of motion

$$\frac{d\hat{x}_I(t)}{dt} = i[H_{\text{int}}^I(t), \hat{x}_I(t)] \quad (32)$$

which can then be expanded as

$$\begin{aligned} \hat{x}_I(t) &= \hat{x} + i \int_0^t d\tau_1 [H_{\text{int}}^I(\tau_1), \hat{x}] \\ &+ i^2 \int_0^t d\tau_1 \int_0^{\tau_1} d\tau_2 [H_{\text{int}}^I(\tau_1), [H_{\text{int}}^I(\tau_2), \hat{x}]] \\ &+ O(H_{\text{int}}^I)^3. \end{aligned} \quad (33)$$

Here $H_{\text{int}}^I(t) = e^{-iH_0 t} \sum_k \lambda_k (b + b^\dagger)(b_k + b_k^\dagger) e^{iH_0 t}$ is the interaction part of the Hamiltonian in the interaction picture. Neglecting all contributions of $O((H_{\text{int}}^I)^3)$ or higher in the perturbative expansion will yield a result that is correct at least to $O(\lambda_k^3)$.

Using the initial state (18), the first order contribution from equation (33) vanishes, since $\langle b_k \rangle = \langle b_k^\dagger \rangle = 0$. Likewise, all odd orders of perturbation theory vanish. Evaluation of the two commutators needed for the second order contribution to $\langle \hat{x}(t) \rangle$ yields

$$\begin{aligned} \langle \hat{x}(t) \rangle &= \sqrt{2}a \cos(\Delta t) - \frac{a}{\sqrt{2}} \int_0^\infty d\omega \frac{4\Delta J(\omega)}{\Delta^2 - \omega^2} \\ &\times \left(-\frac{2\omega}{\Delta^2 - \omega^2} (\cos(\omega t) - \cos(\Delta t)) + \frac{\omega}{\Delta} \sin(\Delta t) t \right) \\ &+ O(\lambda_k^4). \end{aligned} \quad (34)$$

In analogy to our example of naive perturbation theory in classical mechanics from section 2, a secular term occurs in the expansion from equation (34) which leads to large errors on long timescales (see figure 3).

3.3.2. Exact solution. We next derive a closed analytical expression for the quantity $\langle \hat{x}(t) \rangle$ as a benchmark for a full numerical solution of the flow equations. Several other exact results for the dissipative quantum oscillator have been obtained by Haake and Reibold [18]. According to equation (29), we have $\langle \hat{x}(t) \rangle = \sqrt{2}a\beta(0, t)$. The coefficient $\beta(0, t)$ is also given by the commutator

$$\beta(0, t) = \frac{1}{2}[b - b^\dagger, b(t)]_-, \quad (35)$$

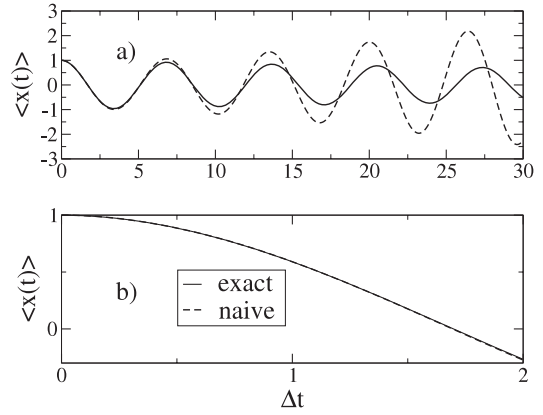


Figure 3. Comparison of the exact solution equation (38) against the naive perturbation theory of equation (34). The secular term occurring in the second order perturbation expansion yields an error growing $\propto t$, see (a). In the short time limit $t \ll 1$, naive perturbation theory becomes exact, see (b). Parameters: $a = \frac{1}{\sqrt{2}}$, $\Delta = 1$; ohmic bath: $J(\omega) = 2\alpha\omega\Theta(\omega_c - \omega)$ with $\alpha = 0.001$, $\omega_c = 10$.

and using the invariance of (35) under the unitary flow (25), we obtain

$$\begin{aligned} \beta(0, t) &= \frac{1}{2}[\tilde{b} - \tilde{b}^\dagger, \tilde{b}(t)] \\ &= 2 \sum_k (\tilde{\alpha}_k^2 + \tilde{\alpha}_k^2) \cos(\omega_k t). \end{aligned} \quad (36)$$

It is possible to evaluate this sum in closed form by defining

$$\begin{aligned} K(\omega) &= \sum_k s_k^2 \delta(\omega^2 - \omega_k^2) \Theta(\omega_c - \omega) \\ s_k &= 2 \left(\frac{\omega_k}{\Delta} \right)^{1/2} \tilde{\alpha}_k = 2 \left(\frac{\Delta}{\omega_k} \right)^{1/2} \tilde{\alpha}_k \end{aligned} \quad (37)$$

what leads to the exact result for the dynamics

$$\langle \hat{x}(t) \rangle = 2\sqrt{2}a \int_0^\infty \omega K(\omega) \cos(\omega t) d\omega. \quad (38)$$

For an ohmic bath with $J(\omega) = \alpha\omega\Theta(\omega_c - \omega)$, the function $K(\omega)$ can be evaluated as

$$\begin{aligned} K(\omega) &= (4\alpha\omega\Delta) \left(16\pi^2 \alpha^2 \Delta^2 \omega^2 \right. \\ &\left. + \left[\Delta^2 - \omega^2 + 8\alpha\Delta \left(-\omega_c + \frac{\omega}{2} \ln \left(\frac{\omega + \omega_c}{\omega_c - \omega} \right) \right) \right]^2 \right)^{-1}. \end{aligned} \quad (39)$$

3.4. Numerical results

In order to illustrate the potential applications of our diagonalization scheme, we calculate the expectation value $\langle \hat{x}(t) \rangle$ by a numerical integration of the flow equations (26). For our numerical calculation, we specify the spectral function of the bath as an ohmic one with a sharp cutoff frequency ω_c .

$$J(\omega) = \alpha\omega\Theta(\omega_c - \omega). \quad (40)$$

This spectral function is discretized with $N = O(10^3)$ states with a constant energy spacing of $\Delta\omega = \frac{\omega_c}{N}$. The systems of coupled differential equations (23) and (26) have to be solved separately for each point in time, since the initial conditions of equation (27) depend on time. For a finite number N of bath modes, the initial conditions for the bath modes have a recurrence time of $T = 2\pi N/\omega_c$, and it is expected that the error blows up rapidly at this timescale. Indeed, we could confirm this behavior numerically. Nevertheless, for times $t < T = O(N/\omega_c)$, a number of about $N = O(10^3)$ bath modes is sufficient to agree with the exact result within an error of less than 1%. The abovementioned features of our numerical calculations are demonstrated in figure 4. Summing up, numerical simulations with only $O(10^3)$ bath states provide excellent agreement with analytical solutions, with finite size effects occurring only at timescales of $O(N)$. In the appendix, we briefly discuss how to efficiently implement our transformation scheme for finite size systems.

4. The dissipative two-level system

The dissipative two-level system

$$H = -\frac{\Delta}{2}\sigma_x + \frac{\sigma_z}{2} \sum_k (b_k + b_k^\dagger) + \sum_k \omega_k b_k^\dagger b_k \quad (41)$$

is a fundamental model for the description of decoherence and dissipation in quantum systems [13, 12]. The two-state system is represented by pseudospin operators σ_i , $i = x, y, z$ and the effect of dissipation is caused by a linear coupling to a bosonic bath. All bath properties can again be modeled by the spectral function $J(\omega)$ defined in equation (17).

Typically, the effect of decoherence manifests itself if the two-level system is prepared in an eigenstate and the coupling to the environment is switched on subsequently. The observable $\langle\sigma_z(t)\rangle$ describes then the tunneling dynamics of the initially pure quantum state.

This problem turns out to be non-trivial and nearly all known results rely on approximations. The approximation scheme of the flow equation approach can be applied to this problem in a controlled way, as shown below. This example demonstrates the ability of our method to treat real-time evolution in non-integrable models without any problems due to secular terms.

4.1. Diagonalization of the Hamiltonian

In order to approximately diagonalize the Hamiltonian (41), we employ the following generator for the unitary flow [19]:

$$\eta(B) = i\sigma_y \sum_k \eta_k^{(y)} (b_k + b_k^\dagger) + \sigma_z \sum_k \eta_k^{(z)} (b_k - b_k^\dagger) + \sum_{kl} \eta_{kl} : (b_k + b_k^\dagger)(b_l - b_l^\dagger) :, \quad (42)$$

with B -dependent coefficients

$$\eta_k^{(y)} = \frac{\lambda_k}{2} \Delta \frac{\omega_k - \Delta}{\omega_k + \Delta}, \quad \eta_k^{(z)} = -\frac{\lambda_k}{2} \omega_k \frac{\omega_k - \Delta}{\omega_k + \Delta}, \quad (43)$$

$$\eta_{kl} = \frac{\lambda_k \lambda_l \Delta \omega_l}{2(\omega_k^2 - \omega_l^2)} \left(\frac{\omega_k - \Delta}{\omega_k + \Delta} + \frac{\omega_l - \Delta}{\omega_l + \Delta} \right).$$

This generator has an important conceptual property that makes it different from the generator (21) used in section 3.4. It does not leave the Hamiltonian form invariant during the flow, since it generates additional interactions. In this case, these newly generated interactions are of $O(\lambda_k^3)$, which we neglect since we consider the couplings λ_k as a small expansion parameter. For more details about the flow equation approach to the spin-boson model we refer the reader to [17]. Due to the expansion in the couplings λ_k , the flow equation calculation in equilibrium is reliable (meaning errors less than 10%) for values $\alpha \lesssim 0.2$ for an ohmic bath.

In the above expressions, normal ordering is denoted by $:\dots:$, which ensures that the truncated higher order interaction terms have vanishing expectation values with respect to the quantum state used for normal ordering. In equilibrium, normal ordering is therefore performed with respect to the equilibrium ground state, $b_k b_{k'}^\dagger =: b_k b_{k'}^\dagger : + \delta_{kk'} n_B(k)$, where $n_B(k)$ is the Bose-Einstein distribution. This procedure is not ideal for real-time evolution of physical observables out of a non-thermal initial state $|\psi_i\rangle$. In order to minimize our truncation error, we define a more general normal-ordering procedure

$$b_k b_{k'}^\dagger =: b_k b_{k'}^\dagger : + \delta_{kk'} n_B(k) + C_{kk'} \quad (44)$$

$$C_{kk'} \stackrel{\text{def}}{=} \langle\psi_i| b_k b_{k'}^\dagger |\psi_i\rangle - \delta_{kk'} n_B(k).$$

Here, the correct non-thermal initial state is used for normal ordering. The flow equations for the Hamiltonian then read:

$$\frac{d\Delta}{dB} = -2 \sum_k \lambda_k \eta_{k'}^{(y)} (1 + 2n_B(k) \delta_{kk'} + C_{kk'})$$

$$\frac{d\lambda_k}{dB} = -(\omega_k - \Delta)^2 \lambda_k + 2 \sum_l \lambda_k \eta_{kl} \quad (45)$$

$$\frac{dE}{dB} = - \sum_k \lambda_k \eta_k^{(z)}.$$

In the limit $B \rightarrow \infty$, the interaction part of the Hamiltonian decays completely and the transformed Hamiltonian is given by

$$\tilde{H} = -\frac{\tilde{\Delta}}{2}\sigma_x + \sum_k \omega_k b_k^\dagger b_k \quad (46)$$

with a renormalized tunneling matrix element $\tilde{\Delta}$. It has been shown in [19] that $\tilde{\Delta}$ obeys the correct universal scaling behavior for ohmic baths [12], $\tilde{\Delta} \propto \Delta(\Delta/\omega_c)^{\alpha/(1-\alpha)}$.

4.2. Real-time evolution of operators

The truncation scheme for the flow of the Hamiltonian (41) can be employed in the same way for the transformation of the spin operators σ_i , $i = x, y, z$. In this section, only the

⁴ The generator (42) is again not the canonical generator in order to leave the flowing Hamiltonian form invariant up to higher orders in the coupling λ_k . It also makes use of the approximation $\langle\sigma_x\rangle = 1$ and neglects small fluctuating parts of this expectation value.

transformations of the operator σ_x are presented. Details of the transformations of the operators σ_y and σ_z are given in the appendix.

An ansatz for the flow of the operator σ_x is formally given by the commutator $[\eta, \sigma_x]$, which contains all contributions to the flow of σ_x which are of first order in the couplings λ_k . For convenience, we parametrize this ansatz for the flowing operator $\sigma_x(B)$ as

$$\begin{aligned} \sigma_x(B) &= h(B) \sigma_x + \sigma_z \sum_k \left(\chi_k(B) b_k + \bar{\chi}_k(B) b_k^\dagger \right) \\ &+ \alpha(B) + i\sigma_y \sum_k \left(\mu_k(B) b_k - \bar{\mu}_k(B) b_k^\dagger \right) \end{aligned} \quad (47)$$

where $\bar{\mu}_k$ and $\bar{\chi}_k$ are related to μ_k and χ_k by complex conjugation. All newly generated terms in the differential equation $\frac{d\sigma_x(B)}{dB} = [\eta(B), \sigma_x(B)]$ are of $O(\lambda_k^2)$ in the coupling constants. These truncated terms are normally ordered according to the convention (44), which finally determines the differential flow of the coupling constants as

$$\begin{aligned} \frac{dh}{dB} &= - \sum_k \left(\eta_k^{(y)} (\chi_k + \bar{\chi}_k) + \eta_k^{(z)} (\mu_k + \bar{\mu}_k) \right) \\ &- 4 \sum_{k,l} \eta_k^{(y)} C_{kl} (\chi_l + \bar{\chi}_l) \\ \frac{d\chi_k}{dB} &= 2h \eta_k^{(y)} + \sum_l (\eta_{kl} (\chi_l + \bar{\chi}_l) + \eta_{lk} (\bar{\chi}_l - \chi_l)) \end{aligned} \quad (48)$$

$$\frac{d\mu_k}{dB} = 2h \eta_k^{(z)} - \sum_l (\eta_{lk} (\mu_l + \bar{\mu}_l) + \eta_{kl} (\mu_l - \bar{\mu}_l))$$

$$\frac{d\alpha}{dB} = \sum_k \left(\eta_k^{(y)} (\mu_k + \bar{\mu}_k) + \eta_k^{(z)} (\chi_k + \bar{\chi}_k) \right)$$

with the initial conditions $h(B=0) = 1$, $\chi_k(B=0) = \mu_k(B=0) = \alpha(B=0) = 0$. In the thermodynamic limit, the observable σ_x decays completely, $h(B \rightarrow \infty) = 0$ [17, 19].

For the application to real-time evolution problems, it is again straightforward to obtain the time-evolved operator $\tilde{\sigma}_x(t)$ by evaluating $\tilde{\sigma}_x(t) = e^{i\tilde{H}t} \tilde{\sigma}_x e^{-i\tilde{H}t}$ with the diagonal Hamiltonian \tilde{H} from (46). It is easy to see that the transformed observable (47) remains invariant under time evolution, and only its coefficients change to time-dependent functions

$$\begin{aligned} \tilde{\chi}_k(t) &= (\tilde{\chi}_k(0) \cos(\tilde{\Delta}t) + i \tilde{\mu}_k(0) \sin(\tilde{\Delta}t)) e^{-i\omega_k t} \\ \tilde{\mu}_k(t) &= (\tilde{\mu}_k(0) \cos(\tilde{\Delta}t) + i \tilde{\chi}_k(0) \sin(\tilde{\Delta}t)) e^{-i\omega_k t}, \end{aligned} \quad (49)$$

where $\tilde{\alpha}$ and \tilde{h} remain unchanged since these contributions commute with \tilde{H} .

The operator $\tilde{\sigma}_x(t)$ with coefficients (49) can be regarded as an effective operator for the calculation of observables in real-time with an error of $O(\lambda_k^2)$. Although this effective operator relies on a perturbative expansion of the flow equations, it is able to correctly describe observables on all timescales, e.g. the error remains controlled also for long times. This property can be understood from the analogy to canonical perturbation theory of classical mechanics, where the Hamiltonian function is first transformed to normal form.

Using equations (48) together with the initial conditions (49), the effective operator $\tilde{\sigma}_x(t)$ can be integrated back

into the initial basis of the problem, thereby inducing a non-perturbative solution of the Heisenberg equation of motion for the operator σ_x , as illustrated in figure 2. Formally, this solution for the operator $\sigma_x(t)$ is given as

$$\begin{aligned} \sigma_x(t) &= h(t) \sigma_x + \sigma_z \sum_k \left(\chi_k(t) b_k + \bar{\chi}_k(t) b_k^\dagger \right) \\ &= \alpha(t) + i\sigma_y \sum_k \left(\mu_k(t) b_k - \bar{\mu}_k(t) b_k^\dagger \right). \end{aligned} \quad (50)$$

After the coefficients $h(t)$, $\chi_k(t)$, $\bar{\chi}_k(t)$, $\mu_k(t)$, $\bar{\mu}_k(t)$, $\alpha(t)$ have been obtained, e.g. by a numerical solution of the flow equations, any desired correlation function of the operator $\sigma_x(t)$ can be calculated.

4.3. Applications

Although it is in principle possible to obtain analytical approximations to flow equations like (48) and (45), we solve the flow equations for the spin operators numerically in this paper. However, these numerical solutions rely on the truncation scheme we introduced above. In order to check the accuracy of this truncation scheme, we first analyze it by comparing it against an exact result.

4.3.1. Comparison against exact results. An exact analytical solution of the spin-boson model can be easily obtained at the so-called pure dephasing point, where $\Delta = 0$. Since σ_z is a conserved quantity in this case, the environment can be traced out analytically. An initial state that contains locally a pure state $|\phi\rangle = \frac{1}{\sqrt{2}}(|\downarrow\rangle + |\uparrow\rangle)$ will become entangled with the environment during the course of time. A measure for this process is given by the decay of the off-diagonal matrix element of the reduced density matrix, $\rho_{\uparrow\downarrow}(t) = \langle \phi | Tr_{\text{boson}} \{ \rho(t) \} | \phi \rangle$, and it was shown [20] that this can be written as $\rho_{\uparrow\downarrow}(t) = \rho_{\uparrow\downarrow} \exp(-\Gamma(t))$ with

$$\Gamma(t) = \frac{1}{\pi} \int_0^\infty d\omega J(\omega) \coth\left(\frac{\omega}{2T}\right) \frac{1 - 2\cos(\omega t)}{\omega^2}. \quad (51)$$

Note that the quantity $\rho_{\uparrow\downarrow}(t)$ is identical to the observable $\langle \sigma_x(t) \rangle$, which can be directly obtained from equation (50). At zero temperature this observable shows a sluggish decay to the ground state expectation value $\langle \sigma_x \rangle_{\text{GS}} = 0$. We now compare this exact result with the flow equation solution at zero temperature. For the given initial state, the quantity $\rho_{\uparrow\downarrow}(t)$ is in the flow equation scheme given by the real function $\alpha(t)$ from equation (50). We evaluate this quantity for ohmic baths with a cutoff frequency ω_c (superohmic baths are also possible, subohmic baths have not yet been treated successfully within our approach). The calculations show that in the regime of low damping strengths $\alpha \leq 0.1$ the agreement with the exact result is excellent, see figure 5. Deviations from the exact result are on all timescales bounded by corrections of $O(\alpha^2)$. The numerical results also show the small transient oscillations of the analytical result, which oscillate with approximately the cutoff frequency. This can be interpreted as a band edge effect which would vanish if a smooth cutoff function like $\exp(-\omega/\omega_c)$ were used for the bath spectrum.

Notice that a numerical solution of the flow equations at finite temperatures (not shown here) is straightforward and also in good agreement with the exact result (51).

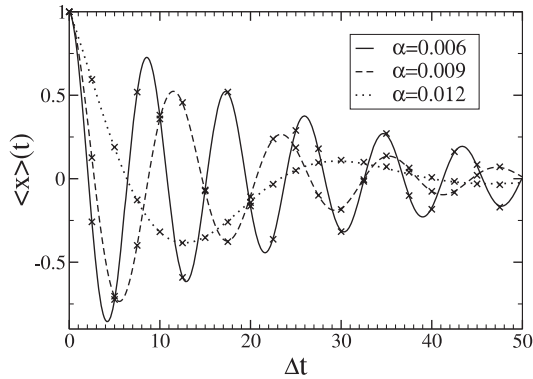


Figure 4. Comparison of the time-dependent displacement $\langle \hat{x}(t) \rangle$ of the dissipative harmonic oscillator, obtained from the analytical result of equation (38) (continuous lines) and numerical integration of the flow equations (crosses). Different damping strengths α have been chosen, and the tunneling matrix element Δ is almost renormalized to zero at $\alpha = 0.012$, leading to a much slower oscillation period. The curve has been normalized to 1 by choosing $a = 1/\sqrt{2}$. The comparison demonstrates that a numerical solution of real-time observables with about 1000 bath states excellently reproduces the analytical result with an error below 1%.

4.3.2. Decay of a polarized spin. The formulation of the spin-boson model was originally motivated by the so-called quantum tunneling problem [12, 13]. In this problem, the two-state system is initially prepared in an eigenstate $|\uparrow\rangle$ of the pseudospin operator, corresponding to a localized state in a double-well potential, which can be reduced to an effective two-state system. The bath, which we again take as ohmic with a frequency cutoff ω_c , is initially in thermal equilibrium and denoted by $|\text{bath}\rangle$. Thus, the initial state $|\psi_i\rangle$ of the total system is given by the product state

$$|\psi_i\rangle = |\uparrow\rangle \otimes |\text{bath}\rangle. \quad (52)$$

After switching on the coupling to the dissipative environment, the time-dependent tunneling dynamics between the two possible states of the two-state system is described by the observable

$$\langle \sigma_z(t) \rangle = \langle \psi_i | \sigma_z(t) | \psi_i \rangle. \quad (53)$$

Within the flow equation approach this is given by the coefficient $z(t)$ from the ansatz (A.5) in the appendix. We have numerically solved the flow equations (A.6) corresponding to the observable (53) and depicted the result in figure 6. As expected, our solutions show long-time stability without secular terms analogous to canonical perturbation theory. For intermediate times, our curves agree well with the well-established NIBA approximation [13, 12], and for long timescales $t \gg \bar{\Delta}^{-1}$ the expectation value $\langle \sigma_z(t) \rangle$ vanishes as expected.

4.3.3. Non-equilibrium correlation functions. Without any additional effort we can also calculate two-time correlation functions based on our non-perturbative solution of the

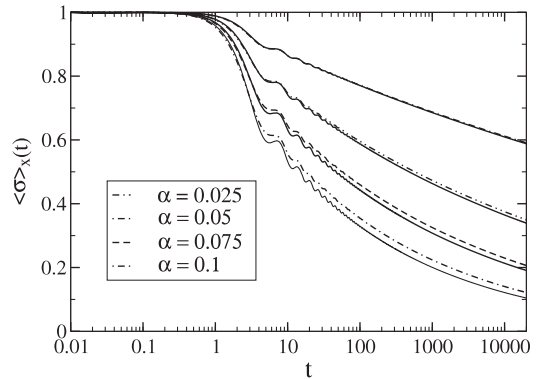


Figure 5. Decay of the off-diagonal matrix element $\rho_{\uparrow\downarrow}(t)$ of the reduced density matrix of the spin-boson model without tunnel splitting ($\Delta = 0$) at $T = 0$. The dashed and dotted lines represent the exact analytical result given by (51), and the full lines the numerical solution of the flow equations. The result demonstrates that the truncation scheme for the flow equations indeed is valid on all timescales, with an error that is systematically controlled in $O(\alpha^2)$. The bath spectral function has been discretized with $N = 30\,000$ states and cut off at $\omega_c = 1$.

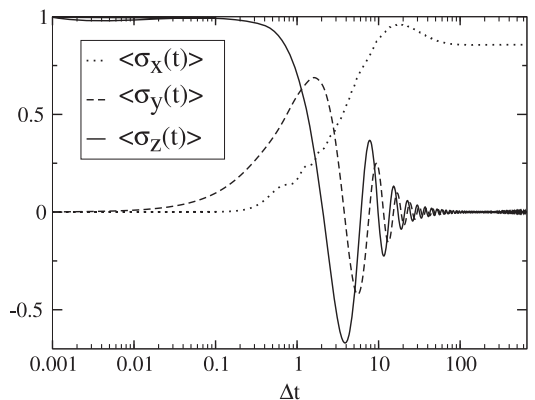


Figure 6. Real-time evolution of the spin expectation values $\langle \sigma_{x,y,z} \rangle(t)$ starting from a polarized spin in the z -direction with a relaxed ohmic bath. We used a damping strength $\alpha = 0.1$ and the parameters $N = 2000$, $\Delta = 1$, $T = 0$ and $\omega_c = 10$.

Heisenberg equations of motion for the spin operators. As an example we discuss the non-equilibrium correlation function

$$S_{zz}(t, t_w) = \frac{1}{2} \langle \{ \sigma_z(t + t_w), \sigma_z(t_w) \}_+ \rangle, \quad (54)$$

where t_w is the waiting time for the first measurement after switching on the dynamics. Notice that in thermal equilibrium this correlation function is time translation invariant and does not depend on the waiting time t_w . It is the relevant quantity for example for neutron scattering experiments [13]. Experimental results for this correlator were, for example, obtained for hydrogen trapped by oxygen in niobium [21], where protons can tunnel between two trap sites of the $\text{Nb}(\text{OH})_x$ sample.

For studying the non-equilibrium dynamics of the spin-spin correlation function, we again use the quantum state $|\psi_i\rangle$ from (52) with the bath at zero temperature as the initial state. Within the flow equation approach, $S_{zz}(t, t_w)$ is readily

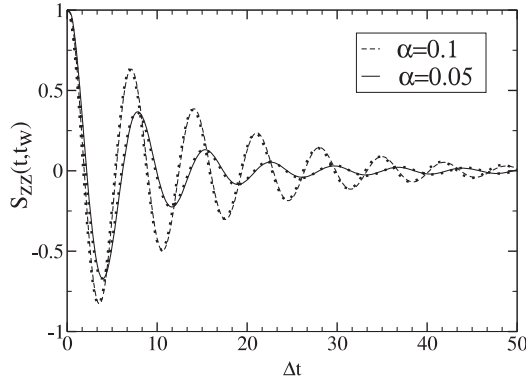


Figure 7. The two-time non-equilibrium correlation function $S_{zz}(t, t_w)$ for two different damping strengths $\alpha = 0.05$ and 0.1 . The full and the dashed line show the result for $t_w = 1$ and the dotted lines correspond to $t_w = 0$. Parameters: $\Delta = 1$, $\omega_c = 10$, $T = 0$, $N = 1000$.

evaluated as

$$S_{zz}(t, t_w) = z(t + t_w)z(t_w) + y(t + t_w)y(t_w) + \sum_k [\bar{\alpha}_k(t + t_w)\bar{\alpha}_k(t_w) + \alpha_k(t + t_w)\alpha_k(t_w)]. \quad (55)$$

All coefficients are explained in the appendix. It turns out from numerical calculations (see figure 7) that the dependence on t_w is only weak in the limit of small damping strengths and the correlations are very close to the equilibrium behavior.

5. Discussion

Our study of real-time dynamics in dissipative quantum systems was motivated by developing an analogous method to canonical perturbation theory, as known from classical mechanics.

Our results show the following. (i) The unitary transformation scheme of the flow equation approach reproduces the well-known advantages of canonical perturbation theory from classical mechanics, especially the absence of secular terms in the time evolution. For example in the spin-boson model, physical observables can be calculated reliably on all timescales since perturbation theory is performed in a unitarily transformed basis. (ii) The identification of a suitable expansion parameter is crucial to obtain reliable results. Notice that the implementation of the flow equation scheme is not restricted to bosonic baths or to impurity models, see e.g. [9, 22]. (iii) Our method is particularly suitable for studying different initial states, since all transformations and approximations are performed on the operator level.

Acknowledgments

We acknowledge financial support through SFB/TR 12 of the Deutsche Forschungsgemeinschaft. AH also acknowledges support through SFB 608 and SK acknowledges support through the Center for Nanoscience CeNS Munich, and the German Excellence Initiative via the Nanosystems Initiative Munich NIM.

Appendix. Additional flow equations for spin operators

A.1. Derivation of flow equations

We briefly provide the flow equation transformations for the spin operators σ_y and σ_z that are constructed in complete analogy to the example from section 4. Using the generator (42), the ansätze for the flowing spin components σ_y and σ_z read

$$\begin{aligned} \sigma_y(B) &= h^{(y)}(B)\sigma_y + i\sigma_x \sum_k \chi_k^{(y)}(B)(b_k - b_k^\dagger) + O(\lambda_k^2) \\ \sigma_z(B) &= h^{(z)}(B)\sigma_z + i\sigma_x \sum_k \chi_k^{(z)}(B)(b_k + b_k^\dagger) + O(\lambda_k^2). \end{aligned} \quad (A.1)$$

The flow equations for these operators are readily derived as

$$\begin{aligned} \frac{dh^{(z)}}{dB} &= \sum_{kk'} \eta_k^{(y)} \chi_{k'}^{(z)} \left(2\delta_{kk'} \coth\left(\frac{\beta\omega_k}{2}\right) + 8C_{kk'} \right) \\ \frac{d\chi_k^{(z)}}{dB} &= -2\eta_k^{(y)} h^{(z)}(B) - 2 \sum_l \eta_{kl} \chi_l^{(z)} \end{aligned} \quad (A.2)$$

and

$$\begin{aligned} \frac{dh^{(y)}}{dB} &= - \sum_{kk'} \eta_k^{(z)} \chi_{k'}^{(y)} \left(2\delta_{kk'} \coth\left(\frac{\beta\omega_k}{2}\right) \right) \\ \frac{d\chi_k^{(y)}}{dB} &= -2\eta_k^{(z)} h^{(y)}(B) - 2 \sum_l \eta_{lk} \chi_l^{(y)}. \end{aligned} \quad (A.3)$$

Next, we solve the Heisenberg equations of motion for the operators $\tilde{\sigma}_y$ and $\tilde{\sigma}_z$, which have the formal solution $\tilde{\sigma}_{y/z}(t) = e^{it\tilde{H}} \tilde{\sigma}_{y/z} e^{-it\tilde{H}}$, with the Hamiltonian \tilde{H} given by equation (46). The solutions read:

$$\begin{aligned} \tilde{\sigma}_y(t) &= \tilde{h}^{(y)}\sigma_y \cos\left(\frac{\tilde{\Delta}}{2}t\right) + \tilde{h}^{(y)}\sigma_z \sin\left(\frac{\tilde{\Delta}}{2}t\right) \\ &\quad + i\sigma_x \sum_k \tilde{\chi}_k^{(y)}(e^{-i\omega_k t} b_k - e^{i\omega_k t} b_k^\dagger) \\ \tilde{\sigma}_z(t) &= -\tilde{h}^{(z)}\sigma_y \sin\left(\frac{\tilde{\Delta}}{2}t\right) + \tilde{h}^{(z)}\sigma_z \cos\left(\frac{\tilde{\Delta}}{2}t\right) \\ &\quad + i\sigma_x \sum_k \tilde{\chi}_k^{(z)}(e^{-i\omega_k t} b_k + e^{i\omega_k t} b_k^\dagger). \end{aligned} \quad (A.4)$$

These operators differ formally from those of equation (A.1), therefore we chose a different ansatz for the transformation of these operators,

$$\begin{aligned} \sigma_{y/z}(B, t) &= \sigma_x \sum_k (i\alpha_k(B, t)(b_k - b_k^\dagger) \\ &\quad + \bar{\alpha}_k(B, t)(b_k + b_k^\dagger) + y(B, t)\sigma_y + z(B, t)\sigma_z + O(\lambda_k^2), \end{aligned} \quad (A.5)$$

which is identical for both σ_y and σ_z . This ansatz yields the time-dependent flow equations

$$\begin{aligned} \frac{d\alpha_k(B, t)}{dB} &= -2y(B, t)\eta_k^{(z)} - 2 \sum_l \alpha_l(B, t)\eta_{lk} \\ \frac{d\bar{\alpha}_k(B, t)}{dB} &= -2z(B, t)\eta_k^{(y)} + 2 \sum_l \bar{\alpha}_l(B, t)\eta_{kl} \\ \frac{dz(B, t)}{dB} &= 2 \sum_k \bar{\alpha}_k(B, t)\eta_k^{(y)} + 8 \sum_{kk'} \eta_k^{(y)} \bar{\alpha}_{k'}^{(z)} C_{kk'} \\ \frac{dy(B, t)}{dB} &= 2 \sum_k \alpha_k(B, t)\eta_k^{(z)} - 8 \sum_{kk'} \eta_k^{(z)} \bar{\alpha}_{k'}^{(y)} C_{kk'}, \end{aligned} \quad (\text{A.6})$$

with the initial conditions

$$\begin{aligned} \tilde{\alpha}_k(t) &= \cos(\omega_k t) \tilde{\chi}_k^{(y)} & \tilde{\bar{\alpha}}_k(t) &= \sin(\omega_k t) \tilde{\chi}_k^{(y)} \\ \tilde{y}(t) &= \tilde{h}^{(y)} \cos\left(\frac{\tilde{\Delta}}{2} t\right) & \tilde{z}(t) &= \tilde{h}^{(y)} \sin\left(\frac{\tilde{\Delta}}{2} t\right) \end{aligned} \quad (\text{A.7})$$

for $\tilde{\sigma}_y(t)$ and

$$\begin{aligned} \tilde{\alpha}_k(t) &= -\sin(\omega_k t) \tilde{\chi}_k^{(z)} & \tilde{\bar{\alpha}}_k(t) &= \cos(\omega_k t) \tilde{\chi}_k^{(z)} \\ \tilde{y}(t) &= -\tilde{h}^{(z)} \sin\left(\frac{\tilde{\Delta}}{2} t\right) & \tilde{z}(t) &= \tilde{h}^{(z)} \cos\left(\frac{\tilde{\Delta}}{2} t\right) \end{aligned} \quad (\text{A.8})$$

for $\tilde{\sigma}_z(t)$. The effective solutions $\sigma_{y/z}(t)$ of the respective Heisenberg equations of motion are now obtained by determining equation (A.5) in the case $B = 0$.

A.2. Numerical implementation of flow equations

In order to numerically integrate a set of $O(10^3) \times O(10^3)$ coupled differential equations, an adaptive step-size fourth order Runge–Kutta algorithm is a fast and accurate choice. Discretizing a bosonic or fermionic bath with equal energy spacing and using about $N = O(10^3)$ bath states yields very accurate solutions up to timescales of $O(N/\omega_c)$. In order to determine initial conditions like equation (A.7), it is sufficient to integrate the flow equations up to $B = O(N^2/\omega_c^2)$, where only a fraction of $O(1/N)$ of the couplings λ_k has not decayed exponentially yet. In order to integrate

flow equations with initial conditions like equation (A.7), a standard Runge–Kutta algorithm does not work properly for large values of the parameter B , since the exponential smallness of the couplings exceeds floating point precision. In our implementation, we therefore stored the flow of the couplings from the diagonalization of the Hamiltonian and supplemented it to the integration of the flow equation with time-dependent initial conditions. Although this procedure cannot use an adaptive step size in order to control the error during integration, it turned out to be very precise in all the cases where we used it.

References

- [1] Greiner M, Mandel O, Hänsch T W and Bloch I 2002 *Nature* **419** 51
- [2] Schollwöck U and White S R 2006 *Effective Models for Low-Dimensional Strongly Correlated Systems* ed G Batrouni and D Poilblanc (Melville, NY: AIP) p 155
- [3] Anders F B and Schiller A 2005 *Phys. Rev. Lett.* **95** 196801
- [4] Anders F B and Schiller A 2006 *Phys. Rev. B* **74** 245113
- [5] Kollath C, Läuchli A M and Altman E 2007 *Phys. Rev. Lett.* **98** 180601
- [6] Manmana S R, Wessel S, Noack R M and Muramatsu A 2007 *Phys. Rev. Lett.* **98** 210405
- [7] Anders F B 2008 arXiv:0802.0371v1
- [8] Hackl A and Kehrein S 2008 *Phys. Rev. B* **78** 092303
- [9] Moeckel M and Kehrein S 2008 *Phys. Rev. Lett.* **100** 175702
- [10] Wegner F 1994 *Ann. Phys. (Lpz.)* **506** 77
- [11] Głazek S D and Wilson K G 1993 *Phys. Rev. D* **48** 5863
- [12] Leggett A J, Chakravarty S, Dorsey A T and Fisher M P A 1987 *Rev. Mod. Phys.* **59** 1
- [13] Weiss U 1999 *Quantum Dissipative Systems* (Singapore: World Scientific)
- [14] See for example: Goldstein H, Poole Ch P and Safko J L 2002 *Classical Mechanics* 3rd edn (Reading, MA: Addison-Wesley)
- [15] See for example: Mahan G D 1990 *Many-Particle Physics* 2nd edn (New York: Plenum)
- [16] Decker H 1981 *Phys. Rep.* **80** 1
- [17] Kehrein S 2006 *The Flow Equation Approach to Many-Particle Systems* (Berlin: Springer)
- [18] Haake F and Reibold R 1985 *Phys. Rev. A* **32** 2462–75
- [19] Kehrein S and Mielke A 1997 *Ann. Phys. (Lpz.)* **6** 90
- [20] Palma G M, Suominen K A and Ekert A K 1996 *Proc. R. Soc.* **452** 567
- [21] Steinbinder D, Wipf H, Magerl A, Richter D, Dianoux A J and Neumaier K 1988 *Europhys. Lett.* **6** 535
- [22] Hackl A and Kehrein S 2008 unpublished